International Journal of Thermophysics, Vol. 26, No. 4, July 2005 (© 2005)
DOI: 10.1007/s10765-005-6708-6

Aerodynamic Levitation and Inductive Heating – A New Concept for Structural Investigations of Undercooled Melts[1]

G. Mathiak,[2,3] I. Egry,[2] L. Hennet,[4] D. Thiaudière,[4] I. Pozdnyakova,[4] and D. L. Price[4,5]

The combined application of containerless techniques with X-ray diffraction and absorption at synchrotron sources as well as neutron diffraction enables structural investigations of high-melting-point and/or corrosive liquids above the melting point and in the undercooled state. A variety of containerless techniques are available including electromagnetic and aerodynamic levitation. In the framework of a bilateral project, a new hybrid system combining aerodynamic levitation with inductive heating is being developed. Advantages and concept of the setup are discussed. Different Helmholtz coils and cylindrical coils were used to heat levitated, solid samples. Melting and stable levitation in the liquid state were achieved for aluminum. The general problem of deformation of liquid samples by electromagnetic fields is discussed.

KEY WORDS: aerodynamic levitation; containerless technique; inductive heating; liquid metals; structural investigations; undercooling.

[1] Paper presented at the Seventh International Workshop on Subsecond Thermophysics, October 6–8, 2004, Orléans, France.

[2] Institut für Raumsimulation, Deutsches Zentrum für Luft- und Raumfahrt e.V., Linder Höhe, 51147 Köln, Germany.

[3] To whom correspondence should be addressed. E-mail: Gerhard.Mathiak@DLR.de

[4] Centre de Recherche sur les Matériaux à Haute Température, CNRS UPR 4212, 1D avenue de la Recherche Scientifique, 45071 Orléans cedex 2, France

[5] Present address: HFIR Center for Neutron Scattering, Oak Ridge National Laboratory, Oak Ridge, Tennessee 37831, U.S.A.

1. INTRODUCTION

Synchrotron radiation has proven to be an important tool for studying microscopic structure in metallic melts. In particular, the combination of containerless techniques with X-ray diffraction at synchrotron sources has enabled structural investigations of high-melting-point and/or corrosive materials above the melting point. Furthermore, deeply undercooled liquid states (100–250 K below the equilibrium melting point) can be reached by containerless methods [1].

The combination of aerodynamic levitation with inductive heating promises an extra degree of control for the investigation of undercooled metallic melts using X-rays and neutrons. Some advantages are expected:

- samples can be processed at low temperatures,
- the temperature of the samples is homogeneous without hot spots,
- the design is compact and the apparatus transportable, and
- stable position of the sample.

The group [2] in Orleans is specialized in aerodynamic levitation and CO_2 laser heating. This heating technique is well adapted for studying liquid oxides and provides good sample stability and temperature control [3]. It can also be used to study metals [4], but it is not optimal in terms of laser power and wavelength.

The group in Cologne is specialized in liquid metal studies using electromagnetic levitation and inductive heating [1, 5, 6]. This method provides homogeneous heating, but the sample is less stable and the temperature control is difficult because the heating depends strongly on the position of the sample in the electromagnetic field. Energy loss occurs by thermal radiation or by additional gas flow cooling.

The two teams have joined their technologies to develop a new hybrid system combining aerodynamic levitation with inductive high frequency heating. This new technique offers the advantages of the two approaches previously used: high sample stability, homogeneous melting, and good temperature control enabling a relatively easy access to the deeply undercooled state of the sample. Due to its compact design, the new hybrid levitator is particularly well suited for implementation at synchrotron or neutron beamlines.

2. CONTAINERLESS PROCESSING

In this section, two containerless techniques, aerodynamic and electromagnetic levitation, and their combination are discussed. The levitated

samples can be heated inductively or by laser radiation, they are cooled convectively by gas flow and, especially at high temperatures, by heat radiation.

2.1. Aerodynamic Levitation

Aerodynamic levitation is a technique based on the use of a gas flow for positioning the sample at a stable position. In this method, samples are levitated by controlling a gas stream flowing through a nozzle. The levitation force results from the pressure p exerted by a jet of velocity v in a gas of density ρ:

$$p = \frac{\rho v^2}{2} \tag{1}$$

In aerodynamic free-jet levitation, a spherical sample is lifted by a fluid jet originating from a nozzle below the sample. Stability in the vertical direction results from the divergence of the jet, which leads to a decreasing drag with increasing height. The levitation force applied on a sphere in the turbulent flow is proportional to the cross-sectional area of the sphere A and to the square of the relative velocity;

$$F = \tfrac{1}{2}\rho C_{\mathrm{D}} A v^2 \tag{2}$$

where ρ is the gas density and C_{D} is the drag coefficient. In principle, the positioning of a liquid droplet in the free jet is difficult [7] because the jet flow is disturbed if the sample changes position or form, and this disturbance is amplified by positive feedback. Lateral positional fluctuations induce destabilizing droplet rotations. The application of free jet positioning of liquid samples without additional stabilizing forces, for example aero-acoustic levitation, is then limited.

The conical nozzle levitator [8] is another method to obtain stable aerodynamic levitation of liquids. The sample is supported by a gas flow passing through a diverging conical nozzle. With this method, the sample is usually laser heated from the top. Temperatures above 3000 K have been obtained with 3-mm-diameter oxide samples [2]. Experimental parameters for the levitation of a sample of given radius r that can be varied are: Reynolds number of the flow, throat diameter, and nozzle geometry (angle and height). In the configuration of Hennet et al. [9, 10], the cone angle is 60°. In a side view, two thirds of the sample can be seen, while the lower third is shaded by the cone. The spherical sample is lifted several tenths of a millimeter in an argon flow of $0.11 \cdot \mathrm{min}^{-1}$. The positioning of a spherical sample is very stable. It is possible to vary flow rate or the density of the sample over a wide range.

This technique can also be used to position or trap drops in microgravity [11, 12]. The conical nozzle in combination with the drop produces expansion in the flowing gas. The Bernoulli forces push the sample back in direction to the throat. This effect is well-known by the textbook experiment where a ping-pong ball is trapped in an inverted funnel. The character of the flow field is very sensitive to the distance between the drop and nozzle, so that especially for higher temperatures the calculation of forces, lateral stability, and the cooling of the sample by the gas flow is very complex.

2.2. Inductive Heating and Electromagnetic Levitation

Electromagnetic levitation, patented by Muck [13] in 1923 and further developed by Okress [14], is a well-known technique for containerless processing of metals and alloys both in the solid and molten states. Levitation and heating is normally achieved by a single conically shaped coil consisting typically of 5–8 windings in the lower section and 1–2 counterwindings in the upper section, powered by a high-frequency power supply. When an alternating current flows through the coil, the alternating electromagnetic field will induce eddy currents within an electrically conducting sample, leading to a repulsive force against the primary electromagnetic field and simultaneously inducing a heating effect. The levitation force is proportional to the gradient of the square of the magnetic field amplitude B, and the heat input is proportional to the square of the magnetic field averaged over the sample surface. The temperature of the sample can be adjusted by heat conduction in an inert gas atmosphere of varying composition or by heat convection with varying gas flow. Molten samples are deformed and stirred by the electromagnetic and gravitational forces.

The main parameter for electromagnetic levitation is the skin depth:

$$\delta = \sqrt{\frac{\rho}{\pi \mu f}}. \tag{3}$$

For an electrical resistivity $\rho = 100\,\mu\Omega \cdot \mathrm{cm}$, magnetic permeability $\mu = 1.25\mu\Omega \cdot \mathrm{s} \cdot \mathrm{m}^{-1}$, and a frequency $f = 300\,\mathrm{kHz}$, the skin depth is $\delta = 0.92\,\mathrm{mm}$. The typical diameter of a levitated sample is in the range of 3–10 mm, and so the zero skin depth approximation is sufficient for many applications.

For nearly spherical samples with effective radius r, the dimensionless quantity,

$$x = \frac{r}{\delta}, \tag{4}$$

determines the heating efficiency.

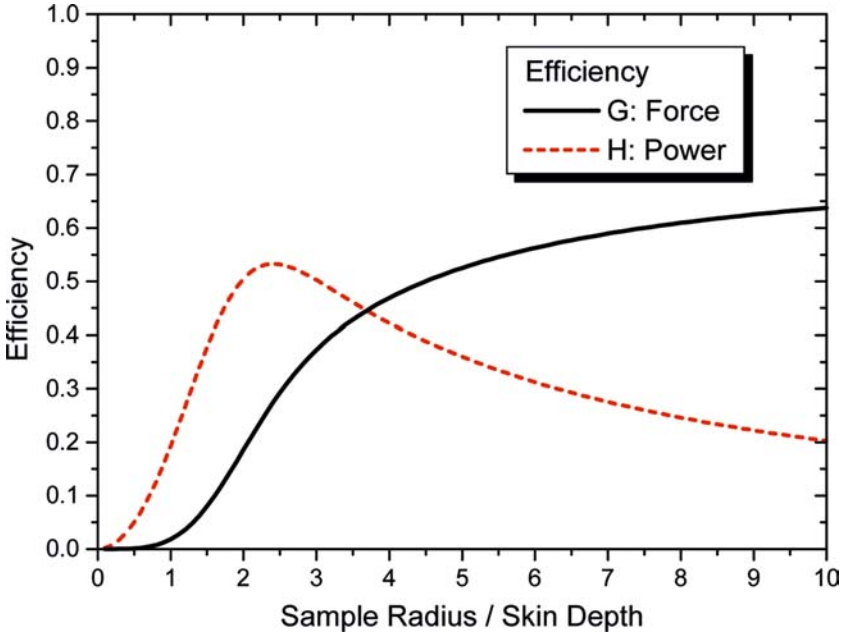

Fig. 1. Efficiency of levitation force and inductive heating as a function of the ratio of sample radius to skin depth.

2.2.1. Levitation Force

Assuming symmetrical loops and a sample diameter much less than the diameter of the coil, and replacing the eddy currents distributed over the whole surface of the sample by a single loop circuit, the levitation force is given by [15]

$$F = -\frac{\nabla(B^2)}{2\mu_0} V G(x) \tag{5}$$

where V is the sample volume and G is the efficiency (see Fig. 1) given by

$$G(x) = \frac{3}{4}\left(1 - \frac{3}{2x}\frac{\sinh 2x - \sin 2x}{\cosh 2x - \cos 2x}\right) \tag{6}$$

For static stability of the sample inside the coil, the levitating electromagnetic force must balance the gravity force. Additionally, it is necessary to have repulsive forces to push the sample back if the sample moves slightly out of the equilibrium position. Especially if the skin depth is very small in comparison to the sample radius, levitated samples can show instabilities resulting in a rotational or oscillatory motion of the sample [16].

2.2.2. Inductive Heating

For a sample diameter that is small in comparison to the coil diameter, the heating power is

$$P = \frac{B^2}{2\mu_0} \omega V H(x) \tag{7}$$

where H is the efficiency (see Fig. 1) given by

$$H(x) = \frac{9}{4x^2} \left(x \frac{\sinh 2x + \sin 2x}{\cosh 2x - \cos 2x} - 1 \right) \tag{8}$$

This function has a maximum at $x = 2.4$.

Normally, levitation coils produce highly inhomogeneous magnetic fields, so that the heating depends strongly on the equilibrium position of the sample, where the levitation force balances the weight of the sample. Therefore, the temperature of the sample cannot be controlled independently by adjusting the coil current. A non-levitating, force-free coil is more suitable to control the temperature of the sample. According to Eq. (8), the skin depth should be $0.6r > \delta > 0.2r$ for high heating efficiency. To optimize force-free coils, the ratio of power (Eq. (7)) to force (Eq. (5)) should be minimized. This requires a high magnetic field amplitude, low magnetic field gradient, high frequency, and low electrical resistivity of the sample. A small sample diameter is incompatible with high heating efficiency because heat loss by radiation or convection is proportional to the surface area while heating is proportional to the volume. For small metallic samples, high frequencies on the order of 100 kHz or more should be used. We have assumed that the sample diameter is much less than the diameter of the coil. In practice, however, it is found that the efficiency of the heating system is much higher when the distance between coil windings and sample is small.

2.2.3. Sample Deformation by Electromagnetic Forces

The shape of a levitated liquid sample is determined by Lorentz forces, hydrostatic forces, surface tension, and, in many applications, aerodynamic forces. The shape of a sample in a vertical axis levitation coil looks like a pear with the tip at the bottom [17]. Even in the absence of gravitational and levitating forces, the heating field of the sample will deform the spherical sample to an ellipsoid with the long axis parallel to the magnetic field.

According to Laplace [18], the capillary pressure,

$$p = \sigma \left(\frac{1}{r_1} + \frac{1}{r_2} \right) \tag{9}$$

of such an ellipsoid is $p = \sigma \frac{2a}{b^2}$ at the pole and $p = \sigma(\frac{1}{b} + \frac{b}{a^2})$ on the equator where a and b are the major and minor axes of the ellipsoid. For nearly spherical samples, the cohesive pressure difference between the top and the equator is

$$\Delta p = 4 \frac{\sigma}{r} \varepsilon \tag{10}$$

where $\varepsilon = (a - b)/b$ and r is the radius of a sphere of the same volume.

This pressure difference is balanced by the magnetic pressure which is the integral over the Lorentz body force, the vector product of the induced eddy current density j with the magnetic field B, perpendicular to the surface. The magnetic pressure is in the approximation of zero skin depth ($\delta << r$),

$$p_m = \int_0^r (\vec{j} \times \vec{B}) d\vec{\rho} = \frac{B_0^2}{4\mu}, \tag{11}$$

on the equator while at the pole, the magnetic field is parallel to the surface normal vector and the magnetic pressure is zero. From the two preceding equations,

$$\varepsilon = \frac{1}{16} \frac{r}{\sigma} \frac{B_0^2}{\mu}. \tag{12}$$

To have spherical samples, ε should be zero, implying that the radius of the sample and the magnetic field should be low, and the surface tension should be high.

This behavior was observed in the microgravity facility TEMPUS with an electromagnetic heating and positioning system for containerless experiments. TEMPUS employs a high-power dipole coil for heating and a lower power quadrupole coil to control sample position. Heating and positioning are decoupled by using two different frequencies [19]. The dipole field is nearly homogeneous in the surrounding of the sample. Nevertheless, when the sample is heated, the sample elongates along the magnetic field and looks like a prolate ellipsoid. The elongation of a sample by a dipole field can be compensated by an additional quadrupole field [20, 21].

2.3. Combination of Aerodynamic Levitation and Inductive Heating

2.3.1. Aerodynamic Levitation Flow Reactor

Winborne et al. [22] described an electromagnetically-stabilized aerodynamic levitation technique for studying gas-liquid reactions. Results for aerodynamically levitated aluminum and uranium have been given. For the levitation of liquid samples they used nozzles with a central hole and six peripheral holes on a circle with a diameter slightly greater than the particle diameter. In a side view, the sample is totally shaded by the nozzle. A 450 kHz current has passed through a simple 30 mm inner diameter, 40 mm long cylindrical coil with five windings without a gap and with the axis parallel to gravity. The sample was placed in the upper section so that there was a small additional levitating force on the sample.

2.3.2. Gas Film Levitation

A particularly interesting system for contactless processing and even shaping of liquids has been developed employing the gas film levitation principle first described by Granier and Potard [23]. A liquid drop is supported by a gas flow from a crucible made of a porous medium. Shaping of liquids in gas layer crucibles is feasible with this technique, using suitably shaped geometries for the crucible.

In the configuration of Haumesser [24], the sample is heated by the gas flow. An electromagnetically heated graphite receptor is used to achieve high temperatures of the gas. So nonconducting samples can be processed and conducting samples are not deformed because the electromagnetic field is concentrated in the receptor and the sample is shaped by the gas flow.

3. DESIGN OF THE APPARATUS

We have developed an apparatus for X-ray absorption and diffraction experiments. For these, good visibility of the sample from the side and high stability during the heating process are necessary.

3.1. Chamber

The chamber for synchrotron measurements (see Fig. 2) consists of a ground plate (180 mm $\times$ 200 mm) with an rf-feedthrough and gas inlet/outlet and a 'bread loaf' shaped cover, made from a 200 mm diameter horizontal cylinder. The cover has flanges for the vacuum system, photodiode (as fluorescence EXAFS detector), beam inlet, pyrometer, and camera for side viewing. Additionally, a 20 mm slit of 120° is cut to provide

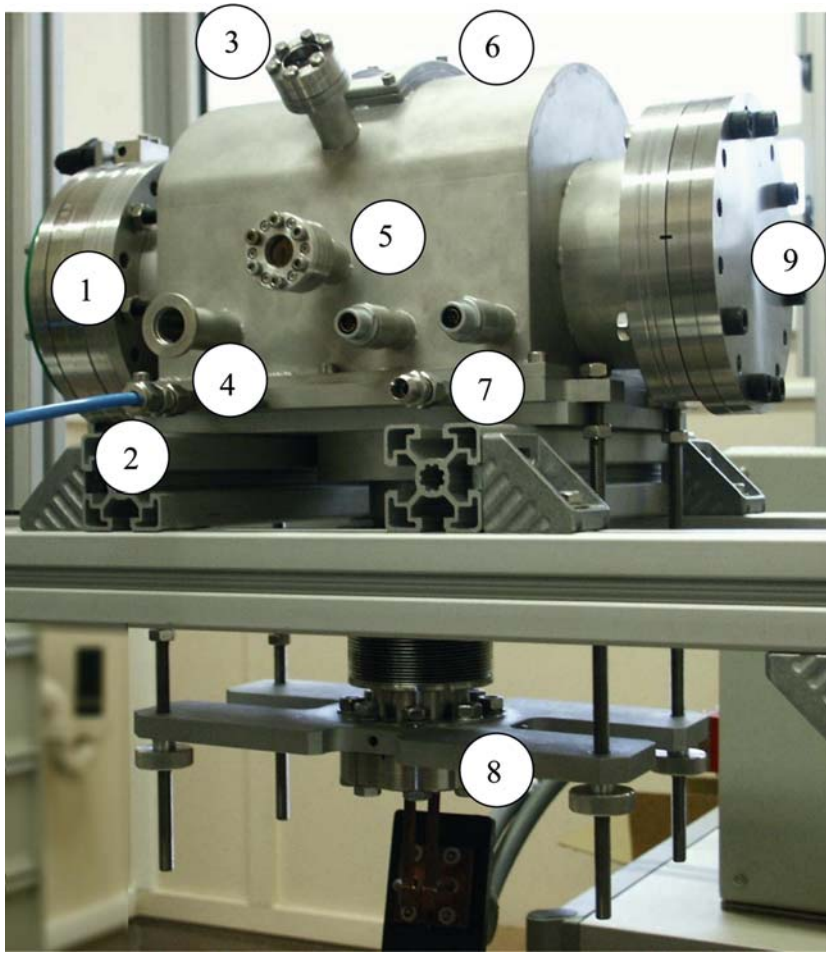

Fig. 2. Photograph of the levitation chamber used for synchrotron radiation measurements. From left to right, the tasks of the flanges are described: 1 – sample exchange, observation; 2 – gas inlet; 3 – pyrometer; 4 – vacuum system; 5 – beam inlet; 6 – slit for the 120° curved detector; 7 – electrical feedthroughs; 8 – high current rf-feedthrough, 9 – photodiode.

an outlet for the diffracted beam. All X-ray windows are sealed with Kapton^{TM}.

The chamber for test measurements is a 120 mm high vertical cylinder with 200 mm diameter. Five standard flanges were used for the pyrometer with an integrated TV camera (top), camera for side view, vacuum, rf-feedthrough for the coil (bottom), and gas inlet/outlet.

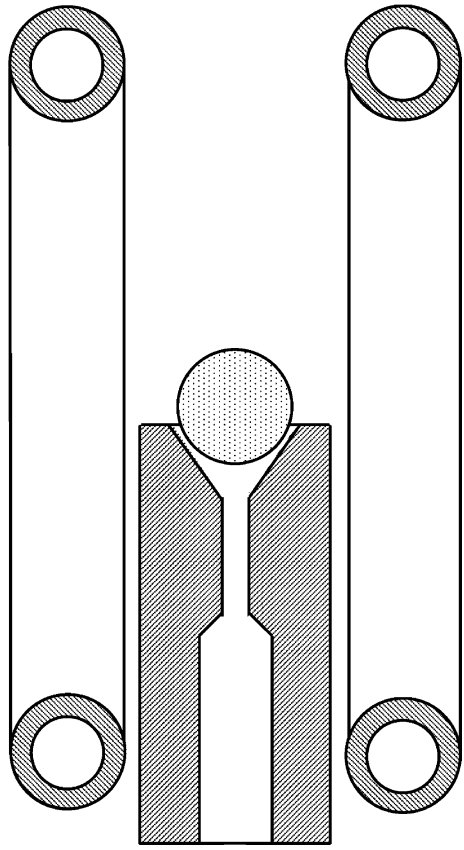

Fig. 3. Sketch of the aerodynamic levitator with inductive heating: The 3 mm sample is levitated inside the convergent-divergent nozzle. On the left and on the right are the windings of the Helmholtz coil with the horizontal axis made of 3 mm copper tube. Consequently, an air gap of 6 mm requires an inner diameter of 15 mm.

3.2. Heating Coil System

As a first attempt, to reach good visibility of the sample and homogeneous field, Helmholtz coils were used (see Fig. 3). This type of coils consists of two windings with an air gap equal to the radius of the coil. The magnetic field amplitudes of coils with different ratios of coil-radius-to-air gap (see Fig. 4) was calculated by integrating Biot–Savart's law, assuming

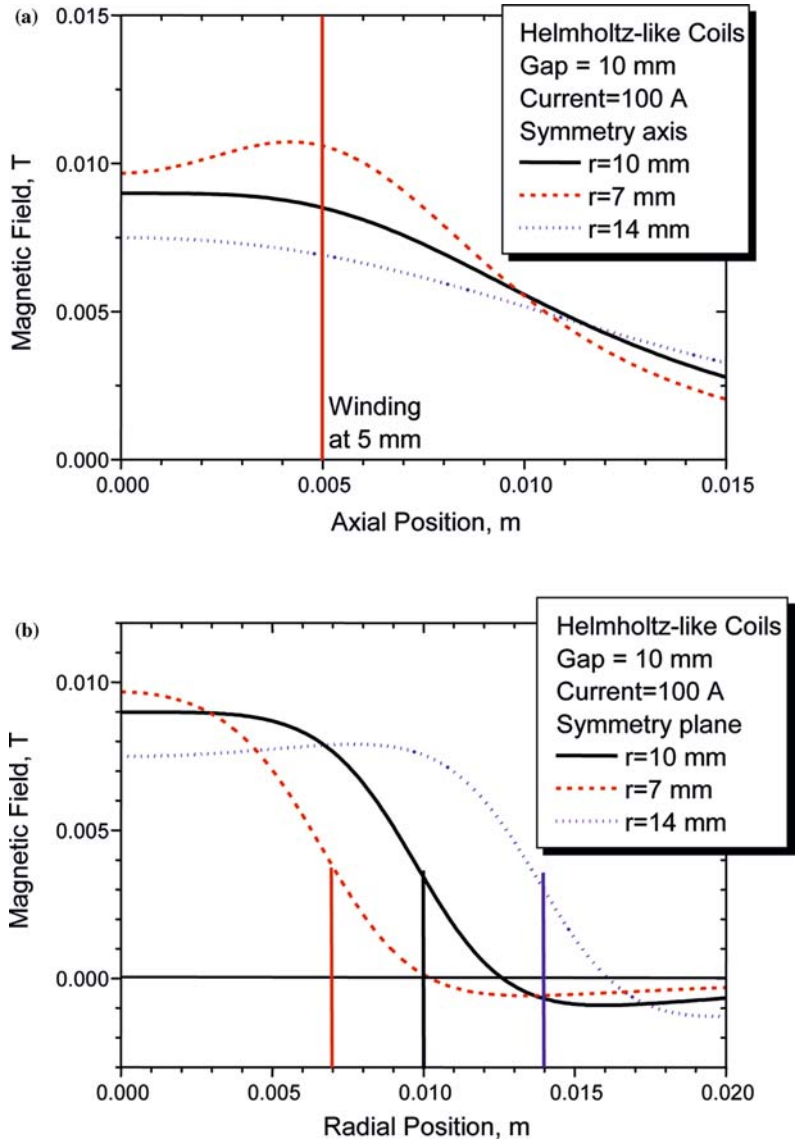

Fig. 4. (a) Magnetic field amplitude B_z ($B_\rho = 0$) along the cylindrical symmetry axis of three Helmholtz-like coils with different ratios of radius to air gap, as a function of the distance to the center. Only the coil with a radius smaller than the air gap has a minimum in the center. (b) Magnetic field amplitude B_z ($B_\rho = 0$) in the symmetry plane of three Helmholtz-like coils with different ratios of the radius-to-air gap, as a function of the distance to the center. Only the coil with a larger radius than air gap has a minimum in the center.

there is no feedback from the sample.

$$\vec{B}(\vec{r}) = \frac{\mu_0 I'}{4\pi} \int \frac{d\vec{s}' \times (\vec{r} - \vec{r}')}{|\vec{r} - \vec{r}'|^3} \tag{13}$$

where $\vec{r}$ is the sample position vector and $\vec{r}'$, I' and $\vec{s}'$ refer to the current-carrying conductor.

Due to cylindrical symmetry, the calculation of the magnetic field vector (B_ρ, B_z, $B_\varphi = 0$) can be simplified in cylindrical coordinates (z, ρ, and φ);

$$B_\rho = \frac{\mu_0}{4\pi} \sum_i I_i R_i \int_0^{2\pi} \frac{(z - z_i)\cos\varphi' d\varphi'}{(\rho^2 + (z - z_i)^2 + R^2 - 2R\rho\cos\varphi')^{3/2}} \tag{14}$$

and

$$B_z = \frac{\mu_0}{4\pi} \sum_i I_i R_i \int_0^{2\pi} \frac{-(\rho\cos\varphi' - R)d\varphi'}{(\rho^2 + (z - z_i)^2 + R^2 - 2R\rho\cos\varphi')^{3/2}} \tag{15}$$

where I and R are the current and radius of a single winding i. The magnetic field was calculated numerically for different aspect ratios of radius

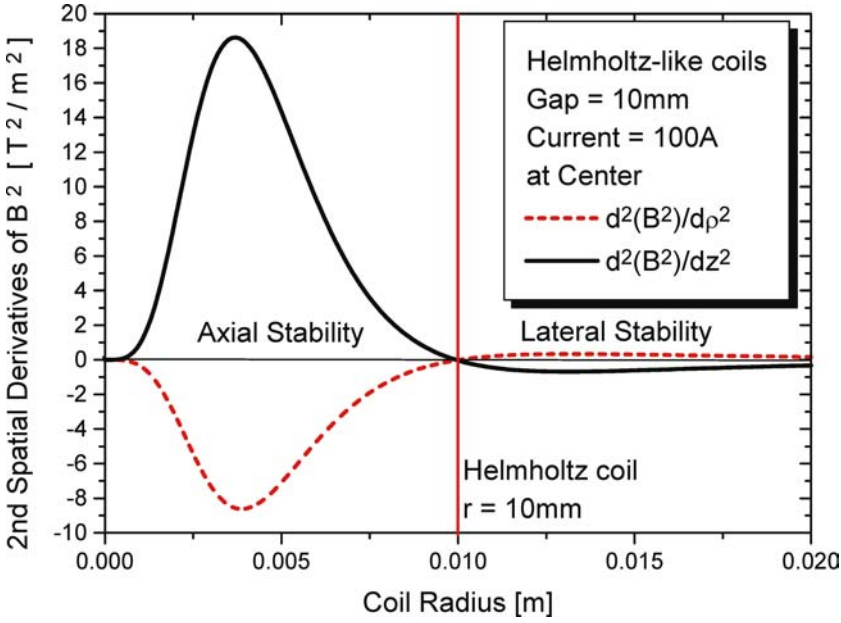

Fig. 5. Helmholtz-like coils: Second spatial derivatives of the square of the magnetic field amplitude at the coil center and the dependence on the coil radius with a constant air gap. There is no coil with stability in the coil center, because the derivatives are inverted.

to distance of the winding pair with infinitesimal small diameter. A Helmholtz coil with equal radius and air gap produces a metastable equilibrium position in the center. In this 'force-free' coil, the magnetic field in the center is nearly constant and suitable for effective heating. For stable positioning, all spatial second derivatives of the square of the magnetic field in the center must be positive. The calculation (see Fig. 5) shows that no Helmholtz-like coil with parallel windings that fulfills these conditions exists. Helmholtz-like coils with the current in the opposite direction are stable in both directions. The magnetic field in the center is zero, so that in this case no heating is possible.

The coils were made out of 3 mm copper tubes and were designed as pairs of 2, 3, or 4 windings. The aspect ratio of radius to distance of the winding pair was chosen to be 1 (Helmholtz-coil), and for comparison 0.7 and 0.4, with strong axial repulsive forces but with lateral instability. The experiments showed that with all three types of coils it was possible to levitate solid samples. All three coils deformed the liquid sample in the same way.

Good heating efficiency and good visibility are contradictory requirements. After first tests with 4 and 10 mm air gaps, 6 mm was chosen. This allows coil configurations with horizontal and vertical axis in combination with a 4 mm diameter nozzle. Horizontal axis coils were used mostly, because this gives the possibility to use a 120° curved detector for diffraction in a vertical plane. This configuration is preferred because of the polarization of the synchrotron beam. Vertical axis coils have the advantage of preserving cylindrical symmetry. For the connection winding between the two coil halves, several designs were tested. Various designs of cylindrical coils with and without air gap were also used in both horizontal and vertical axis directions.

4. TEST EXPERIMENTS

A Hüttinger TIG 5/300 high frequency generator with a maximum power of 5 kW and a frequency of 300 kHz was used for the power supply. The frequency used was approximately 160 kHz, and the power was approximately 70% of maximum.

4.1. Without Levitation

For the first tests of the heating capabilities of the coils, a sample holder was made out of microporous alumina (Kapyrok^{TM}). The first experiments with horizontal axis coils showed that it is possible to melt aluminum, silver, copper, nickel, and zirconium. The copper reacted with

the alumina. The nickel undercooled by a maximum of 30°C. In all cases, solidified samples were elongated in the magnetic field direction.

4.2. With Aerodynamic Levitation

A boron nitride nozzle with 4 mm diameter was designed for 3 mm samples and had a cone angle of 60° and a cone diameter of 3 mm, so that two thirds of the sample can be seen in a side view. Argon was used because of its relatively low thermal conductivity. The flow rate was adjusted between 0.12 and 0.48 $l \cdot min^{-1}$. An addition of 2.5% hydrogen to the gas reduced the oxide surface layer formation of the sample at high temperatures. An oil bubbler was used to maintain atmospheric pressure in the chamber. A disadvantage of argon is its high absorption of X-rays at low energies needed for EXAFS experiments (8 keV).

The coil could be adjusted with solid samples in air. Solid spherical samples (copper, nickel) could be levitated stably over several minutes with small movements, mainly rotation, of the sample inside the cone. Flattened solid samples (cobalt) were stable with the flattened part at the top. Variation of the gas flow produced an effect on the temperature of the solid sample (nickel). With no gas flow the temperature was relatively low because the sample was in direct contact with the nozzle. With increasing gas flow the temperature rose to a maximum because the distance between the sample and nozzle increased. With a further increase of the gas flow, the temperature decreased due to the cooling by the gas flow; eventually the sample became unstable with large amplitude oscillations.

Aluminum samples could be melted and solidified. The pyrometer showed plateaus for melting and solidification (see Fig. 6). The temperature variation between the two plateaus is due to small oxidation of the sample which increased the emissivity. An additional gas purifier will be included in further experiments. No undercooling ($\Delta T < 10$ K) was detectable, which is typical for aluminum. Samples with higher melting temperatures required more generator power for melting. The stronger magnetic field deformed the samples during melting, and often the sample stuck to the nozzle, cooled and solidified immediately. Sometimes, instead of sticking after contact with the nozzle, the liquid sample jumped out of it. This happened with both vertical and horizontal axis coils. Nickel samples were partly melted with a high gas flow rate. The samples were flattened at the bottom, and in addition, a small dimple at the bottom of the solidified sample was observed.

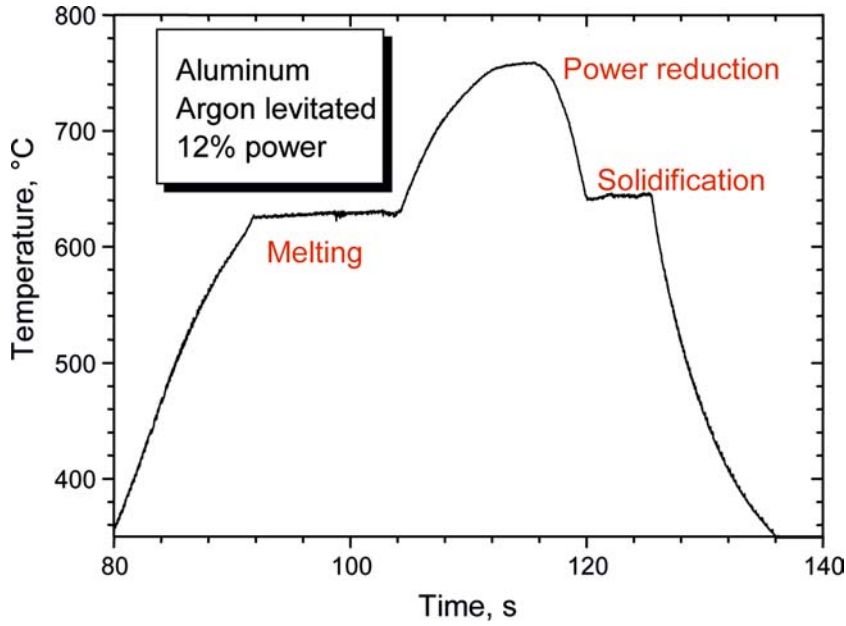

Fig. 6. Pyrometer output without emissivity correction during aerodynamic levitation of aluminum under argon, clearly showing melting and solidification plateaus. The difference of the temperatures of the plateaus can be explained by an increase of emissivity due to oxidation.

5. CONCLUSION AND PROSPECTS

The first results of the new levitation technique look promising. Solid samples can be levitated and heated, showing strong positioning forces of the aerodynamic levitator even when the magnetic field produces repulsive forces. Experiments with liquid aluminum worked well. The open points to be solved are:

- stability and resistance to deformation of liquid or partly liquid samples, and
- undercooling of liquid samples.

Good visibility and high sample stability are conflicting requirements to be satisfied. The levitation system has to be optimized by increasing the aerodynamic or electromagnetic forces to prevent contact between the nozzle and the sample. Enlargement of the nozzle cone, reduction of the throat diameter, and reduction of the cone angle and peripheral holes are possible ways and are under study. Additionally, it is planned to reduce the gas pressure inside the chamber.

ACKNOWLEDGMENT

We want to thank CNRS and DFG for financial support under the bilateral project: "Chemical ordering in high-temperature metallic melts."

REFERENCES

1. D. M. Herlach, R. F. Cochrane, I. Egry, H. J. Fecht, and A. L. Greer, *Int. Mater. Rev.* **38**:273 (1993).
2. J. P. Coutures, J. C. Rifflet, D. Billard, and P. Coutures, *ESA* **SP-256:** 427 (1987).
3. S. Ansell, S. Krishnan, J. K. R. Weber, J. J. Felten, P. C. Nordine, M. Beno, D. L. Price, and M. L. Saboungi, *Phys. Rev. Lett.* **78**:67 (1997).
4. S. Ansell, S. Krishnan, J. J. Felten, and D. L. Price, *J. Phys.: Condens. Matter* **10**:L73 (1998).
5. G. Jacobs and I. Egry, *Phys. Rev. B* **59**:3961 (1999).
6. I. Egry, G. Jacobs, and D. Holland-Moritz, *J. Non-Cryst. Sol.* **250–252**:820 (1999).
7. P. C. Nordine and R. M. Atkins, *Rev. Sci. Instrum.* **53**:1456 (1982).
8. W. A. Oran and L. H. Berge, *Rev. Sci. Instrum.* **53**:851 (1982).
9. L. Hennet, D. Thiaudière, M. Gailhanou, C. Landron, J. P. Coutures, and D. L. Price, *Rev. Sci. Instrum*. **73**:125 (2002).
10. L. Hennet, D. Thiaudière, C. Landron, J.-F. Bérar, M.-L. Saboungi, G. Matzen, and D. L. Price, *NIM* **B 207**:447 (2003).
11. F. Babin, J. M. Gagné, P. F. Paradis, J. P. Coutures, and J. C. Rifflet, *Microgravity Sci. Technol.* **7**:283 (1995).
12. P. F. Paradis, F. Babin, and J. M. Gagné, *Rev. Sci. Instrum.* **67**:262 (1996).
13. O. Muck, *German patent 422004* (1923).
14. E. C. Okress, E. M. Wroughton, C. Comenetz, P. N. Brace, and J. C. K. Kelly, *J. Appl. Phys.* **23**:545 (1952).
15. P. Rony, *Trans. Int. Vacuum Metallurgy Conf.*, M. A. Cocca, ed. (1964), p. 55.
16. J. Priede, G. Gerbeth, A. Mikelsons, and Yu. Gelfgat, *Proc. 3rd Int. Symp. Electromagnetic Processing of Materials*, Nagoya, (2000), p. 352.
17. A. Gagnoud, J. Etay, and M. Garnier, *J. Mec. Theor. Appl*. **5**:911 (1986).
18. P. S. Laplace, *Oeuvres* **4:**389 (1845).
19. J. Piller, R. Knauf, P. Preu, G. Lohöfer, and D. M. Herlach, *ESA* **SP-256**:437 (1987).
20. Y. Asakuma, S. H. Hahn, Y. Sakai, T. Tsukuda, M. Hozawa, T. Matsumoto, H. Fujii, K. Nogi, and N. Imaishi, *Metall. Mater. Trans. B* **31**:327 (2000).
21. H. Fujii, T. Matsumoto, and K. Nogi, *Acta Mater.* **48**:2933 (2000).
22. D. A. Winborne, P. C. Nordine, D. E. Rosner, and N. F. Marley, *Metall. Mater. Trans. B* **7**:711 (1976).
23. J. Granier and C. Potard, *ESA* **SP-256**:421 (1987).
24. P. H. Haumesser, J. Bancillon, M. Daniel, M. Perez, and J. P. Garandet, *Rev. Sci. Instrum.* **73**:3275 (2002).